Journal of Structural Integrity and Maintenance

ISSN: 2470-5314 (Print) 2470-5322 (Online) Journal homepage: http://www.tandfonline.com/loi/tstr20

Seismic incidence on base-isolated nuclear power plants considering uni- and bi-directional ground motions

Thanh-Tuan Tran, Thi-Huong Nguyen & Dookie Kim

To cite this article: Thanh-Tuan Tran, Thi-Huong Nguyen & Dookie Kim (2018) Seismic incidence on base-isolated nuclear power plants considering uni- and bi-directional ground motions, Journal of Structural Integrity and Maintenance, 3:2, 86-94, DOI: 10.1080/24705314.2018.1461547

To link to this article: https://doi.org/10.1080/24705314.2018.1461547

JOURNAL OF STRUCTURAL INTEGRITY AND MAINTENANCE, 2018
VOL. 3, NO. 2, 86–94
https://doi.org/10.1080/24705314.2018.1461547

Taylor & Francis
Taylor & Francis Group

Seismic incidence on base-isolated nuclear power plants considering uni- and bi-directional ground motions

Thanh-Tuan Tran, Thi-Huong Nguyen and Dookie Kim

Department of Civil Engineering, Kunsan National University, Gunsan-si, Korea

ABSTRACT

The effects of bi-directional ground motions of the input seismic on base-isolated Nuclear Power Plants are investigated by comparing to the responses under uni-directional ground motion. For this aim, an analytical model is used to calculate the incidence angle (IA) of ground motions that vary from 0 to 360 degrees, with the interval of 15 degrees, and to show their effects on diverse engineering demand parameters. The observed responses corresponding to the displacement, the rotation and the element force are determined. In addition, the critical angles of the structure under two components with respect to one component are obtained. It is found that the maximum responses of the base-isolated structure for individual records may be decreased at some angles while increased at other angles. In case of bi-directional ground motions, the effect of IA is less considerable than uni-directional ground motion. Moreover, the critical responses under bi-directional seismic excitations are more adequate than uni-directional one. The displacement and shear force responses from one component are less than corresponding values from two components.

KEYWORDS

Incident angle; base-isolated nuclear power plants; critical angle; earthquake response; bi-directional ground motions

Introduction

In seismic design, the earthquake excitation records should be applied in any directions to get a more accurate estimation of structural execution and damage. Normally, earthquake ground motion data are recorded along three directions, two horizontal and one vertical component which considered as correlated processes. However, in the work by Penzien and Watabe (1974), there is a set of principal directions which the ground motion components are uncorrelated. The horizontal axis is considered as major direction and the vertical axis is considered as minor direction. These directions are non-orthogonal and utilized for determining the critical angle that causes the maximum response of engineering demand parameters (EDPs). The angle between the reference directions of the structure and the principal directions of ground motion is called the incident angle (IA). Later, several authors studied the effect of seismic incidence on several EDPs for symmetric and asymmetric building (Lagaros, 2010; Rigato & Medina, 2007). Nguyen and Kim (2013) consolidated the essential of IA in the inelastic range of asymmetry single-storey building's behavior. Kim et al. (2016) provided a seismic evaluation method based on modal energy balance concept for different building structures. Sharmin, Hussan, Kim, and Cho (2017) have evaluated the responses of jacket supported offshore wind turbine (OWT) under seismic incident excitations considering soil–structure interaction. Obtained results indicate that most of the structural models attain the maximum response at any angle other than orthogonal angles as 0°, 90°, i.e. of the ground motions. Soltani, Shakeri, and Zarrati (2018) developed a model of risk management for power tunnels in Iran. Ghersi and Rossi (2001) demonstrated inelastic behavior of in plan irregular system when bi-directional seismic ground motions applied; in most cases, the adoption of Eurocode 8 provisions allows the limitation of orthogonal elements ductility demand.

To examine the critical angle, Smeby and Der Kiureghian (1985) proposed a response spectrum method which is based on fundamental concepts of stationary random vibration with the wideband input process. In this study, the correlation between modal responses and input components was given. López and Torres (1997) also proposed a method to evaluate the critical angle under two ground motion records. Several combination rules, i.e. 30, 40% and CQC3, have been investigated to calculate the maximum response of the structure (Kostinakis, Athanatopoulou, & Tsiggelis, 2013 and Lopez, Chopra, & Hernandez, 2000). Tsourekas and Athanatopoulou (2013) studied the structural response under three ground motion components showing that the response produced by using the analysis suggested in Nuclear Regulatory Guide is smaller than maximum ones overall incident angles.The GCQC3 rule (Hernández & Lopez, 2003) has modified from CQC3-rule to calculate the maximum and minimum responses to horizontal and vertical components. Some studies about SRSS modal combination rule (Heredia-Zavoni, 2011) were also presented in seismic analysis. Valdés-González, Schroeder, and Martínez (2015) show the problem of seismic effects considering IA when simultaneously ground accelerations applied. Menun and Der Kiureghian (2000a, 2000b) developed a response spectrum based on the process of assessing the envelope that bounds two or more responses in a linear structure. Athanatopoulou (2005) developed an analytical formula that utilized for the elastic asymmetric structure to define the seismic critical incidence angle. In this paper, the correlation between modal responses and input components was given.

CONTACT Dookie Kim kim2kie@kunsan.ac.kr

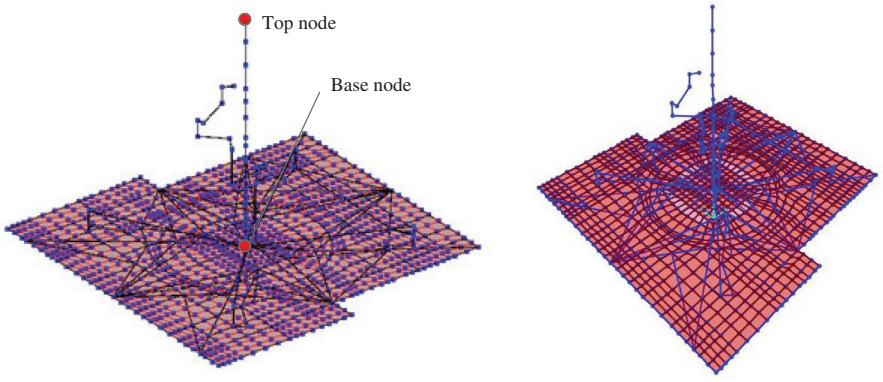

a. OpenSees model b. Sap2000 model

Figure 1. Nuclear island of the APR1400 plant model.

Other researchers have studied on Nuclear Power Plants (NPPs). The probabilistic seismic hazard analysis (PSHA) of Wolsong site on Korea peninsula for Base-isolated NPPs (BI-NPPs) was investigated by Ali et al. (2014). The effects of spatial variation of earthquakes in a hard rock site on the seismic responses of BI-NPPs with lead rubber bearing (LRB) are observed by Sayed et al. (2015). Chang et al. (2016) proposed a Stockbridge damper which can reduce the seismic response of NPPs piping system. Several discussions about platform model of soil–structure system used for the analysis soil–structure interaction controlling seismic response of NPP structure have been presented in the work by Tyapin (2016). Ali et al. (2017) evaluated the seismic response of BI-NPPs under the long-period ground motions and the short-period ground motions. It can be seen that base isolation plays an important role in reducing the structural responses on NPPs. However, when IA is deliberated, the effects on BI-NPPs have to be considered more carefully.

The objective of this research is to assess the behavior of the BI-NPPs structure under IA of uni-directional and bi-directional ground motions. Pairs of horizontal acceleration excitations of two seismic records are matched to the response spectral shapes of NRC (Nuclear regulatory commission) and EUR (European Utility Requirements). Critical angles and maximum relative deviation of responses are obtained when horizontal components are applied separately and simultaneously.

Model of base-isolated nuclear power plant

Super-structure model

Archetype Nuclear Test model (ANT) super-structure of Korean APR1400 nuclear island focuses on the behavior and analysis result of isolators is considered. The geometry dimensions in plan are 103.6 m × 102.4 m (340.0 ft × 336.0 ft) with 445 pedestals. The dimension ($W \times D \times H$) of the pedestals is 2.44 m × 2.44 m × 1.80 m (8.0 ft × 8.0 ft × 5 ft − 11 in).

The numeral model of ANT has been modeled as a simplified stick model (Figure 1(a)) incorporating an equivalent isolator model using the OpenSees software framework. The details of equivalent bearing are described in Table 1. The ANT numerical model includes the Nuclear Island (NI) buildings, the bearings supporting the nuclear island, bearing pedestals, and a lower basemat. The NI in Figure 2 includes reactor systems, internal structures and containment structures of reactor containment building (RCB), auxiliary complex building (ACB), and an upper basemat supporting the RCB and ACB. For the purposes of this benchmark, the upper basemat is considered to be rigid. Dynamic responses such as displacement, rotation, and base shear are used to evaluate the importance of incident angles of a ground motion inelastic range of structural behavior.

Table 1. Bearing properties of base isolator (one-bearings equivalent model).

	Linear		Nonlinear		
Direction	Stiffness	Damping	Stiffness	Yield strength	Post yield stiffness ratio
X	4.296E+08	528990.10	–	–	–
Y	298,846.26	65,728.58	17,906,359	110,312.28	7.820E-03
Z	298,846.26	65,728.58	17,906,359	110,312.28	7.820E-03
XX	5.162E+09	1.140E+09	–	–	–
YY	3.383E+12	3.831E+06	–	–	–
ZZ	4.037E+12	4.595E+06	–	–	–

Verification of numerical model

Finite element Models (FEM) are important for predicting the natural behavior of complex structures with and without unusual loading, and can be conducted to assess the seismic capabilities of such structures. The fundamental natural frequencies of fixed NPP are 3.858 Hz, 3.859 Hz, and 5.077 Hz for 1st, 2nd, and 3rd modes, respectively. In order to verify the OpenSees model, the finite element model of ANT with SAP2000 in Figure 1(b) is presented. Table 2 lists the natural frequencies of structure with the isolator systems identified by OpenSees and SAP200 results. As seen, the OpenSees FEM natural frequencies have a good agreement with the frequencies SAP2000 model. The observation leads to clear verification of the OpenSees model.

Ground motion

Two spectral shapes in Figure 3 are included in the linear dynamic, namely EUR (European Utility Requirements 2.4.6 for hard soil, European utility requirements for LWR Nuclear Power Plants (2002) and NRC (US-NRC Regulatory Guide 1.60, U.S. Nuclear regulatory commission office of Nuclear regulatory research (US Nuclear Regulatory Commission, 1973). Loma Prieta and Imperial Valley earthquake data are matched to EUR and NRC, respectively.

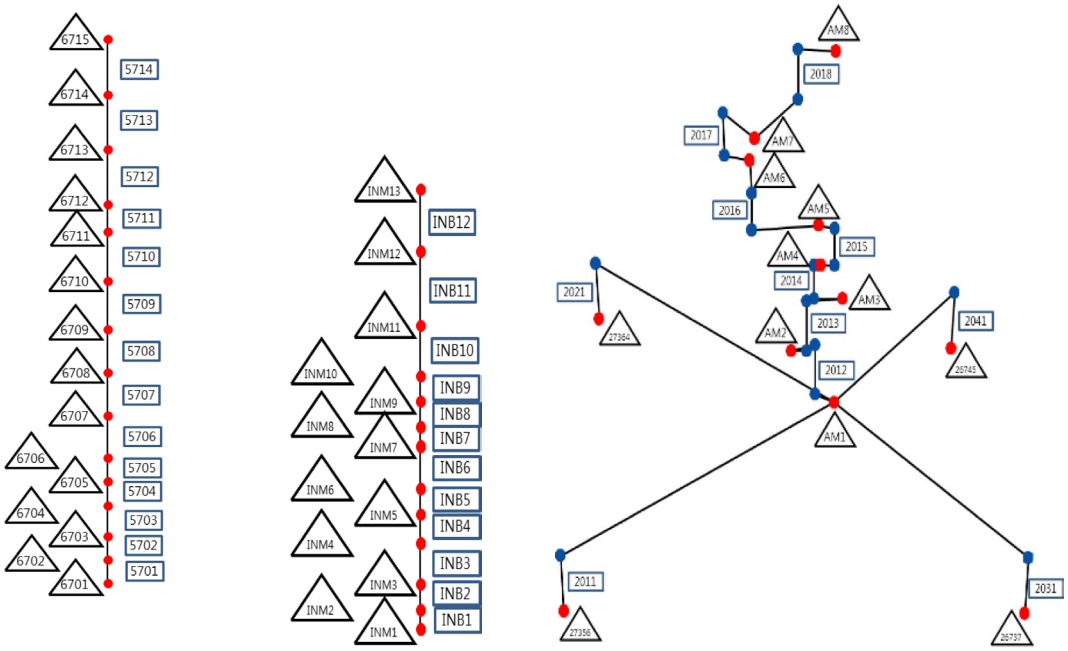

a. RCB b. Internal Structure c. ACB

Figure 2. Nuclear island of the APR1400 plant: different components of stick model.

Table 2. The natural frequency of FEM of the BI-NPPs structure (Hz).

Mode	Description	SAP2000	OpenSees
1	1st translational	.477	.477
2	2nd translational	.477	.477
3	1st torsional	.710	.710

Methodology

The analyses are performed considering the impacts of one horizontal component and two horizontal orthogonal components of the selected ground motions, respectively. The former one is the uni-directional ground motion (Rigato and Medina, 2007) that is the major component only, and the later ones are the bi-directional ground motions (Rigato and Medina, 2007) that are composed of the major and minor components. Therefore, called X and Y the principal axes of the structure, the major and minor components are additionally rotated θ away from the X axis. The angle θ is defined an orientation of the two horizontal excitation axes ($X, X\prime$). With the major and minor components scaled, the major component was applied at various angles of incidence, θ, while the minor component is applied at an angle of $\theta + 90°$ with respect to the x-axis.

The responses due to the major and the minor ground motion components are applied to calculate the critical responses of the NPPs in the case of uni-directional ground motion. On the other hand, for bi-directional ground motions, the maximum responses to the orthogonal seismic components at time instants, t, $\theta = 0$ are computed using mean spectra for the major and the minor components of the selected ground motions by the well-known formula SRSS rule as shown in

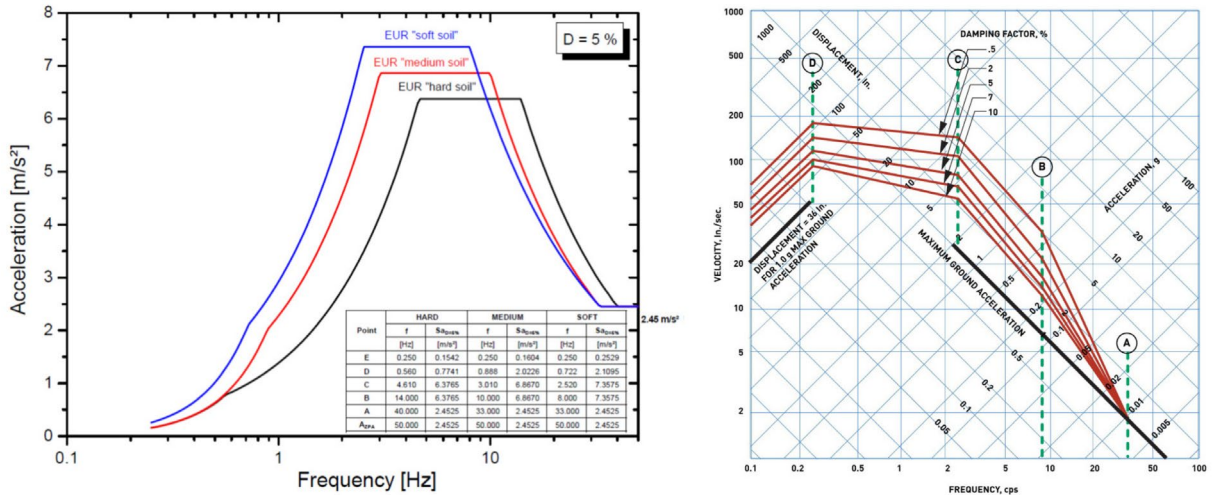

a. EUR (EUR, 2002) b. NRC (US Nuclear Regulatory Commission, 1973)

Figure 3. Spectral shape of EUR and NRC.

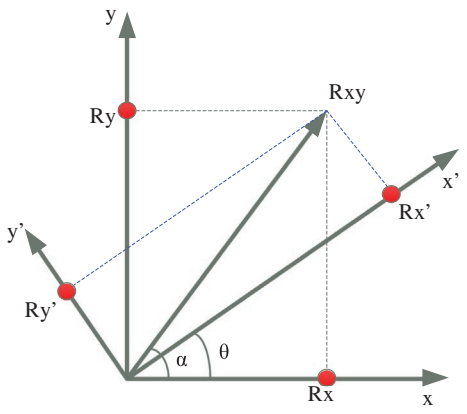

Figure 4. Vectorial representation of R_x and R_y

Figure 4. A simplified process for considering the influence of seismic incidence of structures subjected to ground motion components is discussed in this study and summarized in the following:

For the multi degree of freedom system, the equation of motion is shown by Equation (1)

$$\mathbf{M}\ddot{u}(t) + \mathbf{C}\dot{u}(t) + \mathbf{K}u(t) = -\mathbf{P}_{\text{eff}}(t) \tag{1}$$

where: **M**, **C,** and **K** are the mass, damping, and stiffness matrices of the structure, respectively; $u(t)$, $\dot{u}(t)$ and $\ddot{u}(t)$ are the displacement, velocity, and acceleration vectors of structural response, respectively; $\mathbf{P}_{\text{eff}}(t)$ is the earthquake effective force vector, which can be described by Equation (2)

$$\mathbf{P}_{\text{eff}}(t) = -\mathbf{M}[I_{EW}\ddot{u}_{EW}(t) + I_{NS}\ddot{u}_{NS}(t)] \tag{2}$$

where I_{EW} and I_{NS} are the influence vectors joining the degrees of freedom of the structure to the ground motion components; $\ddot{u}_{EW}(t)$ and $\ddot{u}_{NS}(t)$ are the two rotationally transformed horizontal components of $\ddot{u}_x(t)$ and $\ddot{u}_y(t)$ along the reference axes east–west (EW) and north–south (NS) directions. In Figure 4, $R_x(t)$ and $R_y(t)$ are the instantaneous responses in the x and y directions, respectively. Therefore, the typical response quantity R_{xy} is denoted as follows:

$$R_{xy}(t) = \sqrt{R_x^2(t) + R_y^2(t)} \tag{3}$$

When $\theta \neq 0$, the response of structure along each component is computed as:

$$R'_x(\theta, t) = R_{xy}(t)\cos[\alpha(t) - \theta] \tag{4}$$

$$R'_y(\theta, t) = R_{xy}(t)\sin[\alpha(t) - \theta] \tag{5}$$

where $R'_x(t)$ and $R'_y(t)$ are the responses of structure in the $x\prime$ and $y\prime$ directions, respectively, and $\alpha(t) = \tan^{-1}\left(\frac{R_y(t)}{R_x(t)}\right)$

Because of the cosine function, the maximum response in each direction is limited by condition:

$$-R_{xy}(t) \le R'_x(\theta, t) \le R_{xy}(t) \tag{6}$$

$$-R_{xy}(t) \le R'_y(\theta, t) \le R_{xy}(t) \tag{7}$$

Critical angle θ_{cr} occurs at time critical t_{cr} with the largest peak response (global maximum value):

$$\max R'_x(\theta, t) = R_{xy}(t_{cr}) \tag{8}$$

$$\theta_{cr} = \alpha(t_{cr}) = \tan^{-1}\left(\frac{R_y(t_{cr})}{R_x(t_{cr})}\right) \tag{9}$$

The relative error is considered in the determination of the influence of incidence angle on uni-directional and bi-directional seismic excitations.

$$r_x \text{relative error} = \frac{R'_x(\theta_i, t) - R_x^{\text{median}}}{R_x^{\text{median}}} \tag{10}$$

$$r_y \text{relative error} = \frac{R'_y(\theta_i, t) - R_y^{\text{median}}}{R_y^{\text{median}}} \tag{11}$$

R_x^{median}

$$r_{xy} \text{relative error} = \frac{R'_{xy}(y\theta_i, t) - R_{xy}^{\text{median}}}{R_{xy}^{\text{median}}} \tag{12}$$

where θ is the orientation of the two horizontal excitation axes with respect to the structure reference axes; $R'_x(\theta_i, t)$, $R'_y(\theta_i, t)$, and $R'_{xy}(\theta_i, t)$ are the value of responses for an IA $\theta = \theta_i$, respectively; and, R_y^{median}, R_{xy}^{median} are the median value of responses when the input records are aligned with the structure reference axes $\theta = 0$.

Result and discussion

Earthquake analysis

In this section, two horizontal seismic ground motion components are applied separately to evaluate the response of EDPs of NPPs. Loma Prieta and Imperial Valley earthquakes are considered to indicate the difference of displacement, rotation, and shear force behavior in BI-NPPs structure.

Impact of earthquake on BI-NPPs displacement

In Figure 5, the displacement responses of BI-NPP at top node in each direction are displayed. As seen these values in x and y directions are .210 and .283 m, respectively, under Imperial Valley; for the Loma Prieta, the responses are .0407 and .0463 m in the same directions. When the base isolation system is not considered, the displacements under Imperial Valley are .0164 and .0160 m for x and y axes and for Loma Prieta .336 × 10^{-3} and .434 × 10^{-3} m, respectively. Although there is an increasing amount of displacement at top node of structure, the relative displacements have a minor change as shown in Figure 6. Figure 7 illustrates the maximum displacements of different nodes subjected to seismic excitation in each horizontal direction considering the effects of IA. It is evident that responses are almost repeated after 180° at two horizontal axes of the earthquakes; the responses increase from base to top node at both excitations. The maximum responses at top node under Imperial Valley in x and y directions are .288 and .294 m, respectively, exceeding the results in Loma Prieta, which are only .058 and .049 m for the same directions. The variation of the maximum and minimum displacement of the base-isolated structure from different angles is considered. In case of Loma Prieta earthquake, the variations at the top node are found to be 54.09 and 40.02% for the x and y directions, respectively, while the values at the top for Imperial Valley are 94.97 and 104.26% for the same directions.

The effects of the IA on the structural response at the top node are higher than at the base node. As can be seen in Figure 7, the increasing amounts of maximum displacement

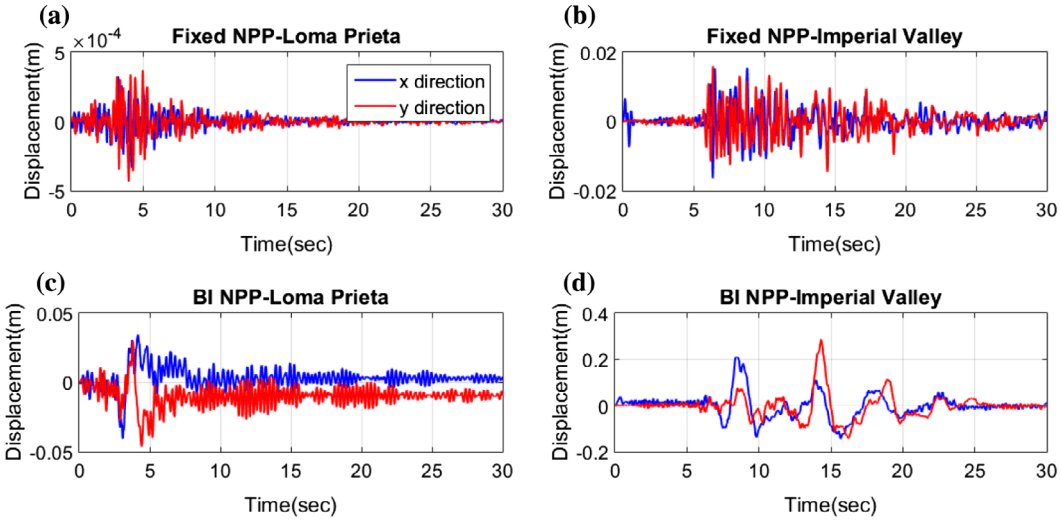

Figure 5. Displacement response at top node of fixed NPP (a–b) and BI-NPPs (c–d).

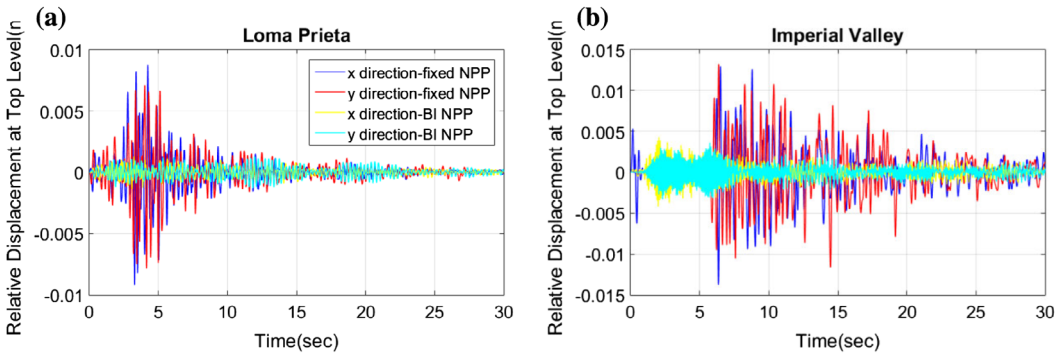

Figure 6. Relative displacement under different earthquakes.

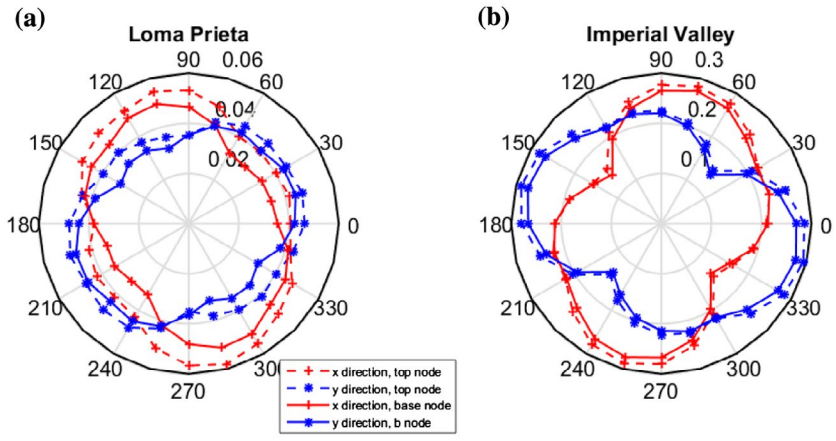

Figure 7. BI-NPPs displacement at top and base node under different earthquakes.

under Loma Prieta are 30.1 and 26.6% for *x* and *y* directions, respectively, while they are 11 and 7.8% in the same directions under Imperial Valley. In addition, the *x* direction result is more considerable than *y* direction in Loma Prieta and the opposite performance is for Imperial Valley record. Besides, the critical incidence angle depends on the direction of ground motion records and each different earthquake. Under earthquake records of Loma Prieta, the critical angles are 285° together with 185°, compared to 255° and 345° for Imperial Valley.

Impact of different earthquakes on rotation response of BI-NPP

The results in Figure 8 show the maximum rotation responses of BI-NPPs under two earthquakes. In general, the response shapes from base to top node in each direction are identical and results from Imperial Valley are more considerable. Maximum rotation at *x* axis of Imperial Valley is 4.72×10^{-4}rad which is almost three times bigger than Loma Prieta (1.63×10^{-4}rad). Along the *y* axis, the results are 4.89×10^{-4}rad for Imperial

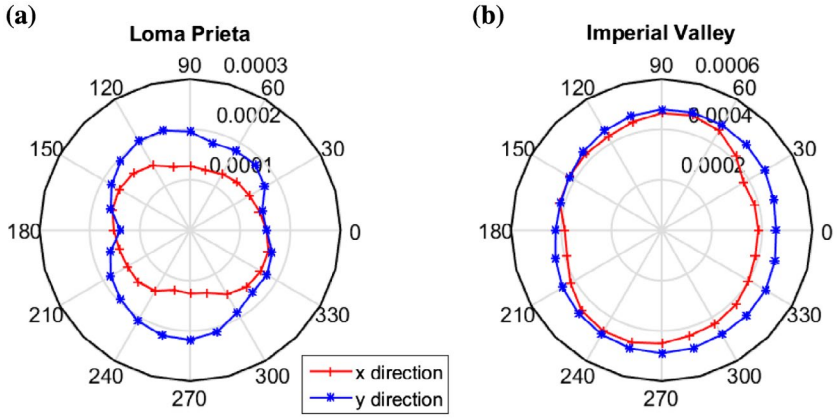

Figure 8. BI-NPPs rotation under different earthquakes.

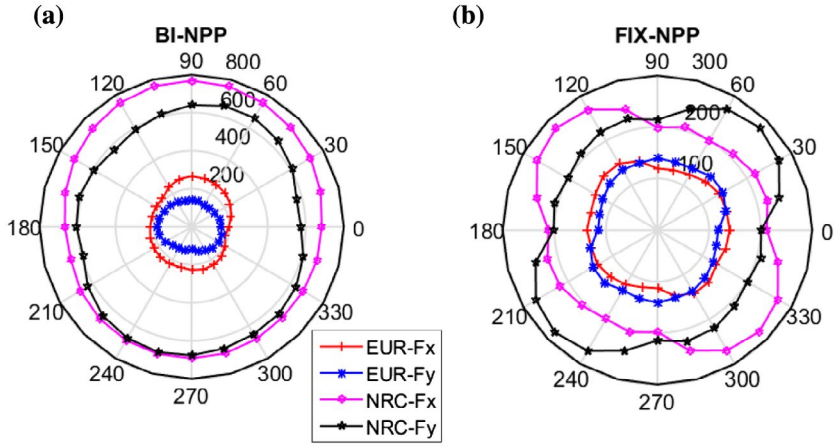

Figure 9. Maximum shear forces in fixed and BI-NPPs model (10^6N).

Valley and 2.18×10^{-4}rad for Loma Prieta. It can be seen that the ratio between them is more than two times.

Impact of earthquakes on shear force of BI-NPP

Figure 9 shows the different shear force responses between Fixed NPPs and BI-NPPs models under different ground motions at element 5701 – the first element of RCB (Figure 2(a)) from the base node. It is clear that in case of BI-NPPs model, the response changes for different angles are almost negligible, while in case of the fixed model the response is repeated after 180°. The maximum values of BI-NPPs under NRC are 7.69×10^5 kN for x direction at 90° and 6.82×10^5 kN for y direction at 255°; whereas these results for EUR are 2.66×10^5 kN together with 1.8×10^5 kN in x and y directions, respectively. The maximum relative variation along x and y axes under Imperial Valley is 45.12 and 48.34% for BI-NPPs. Meanwhile, the proportion of fixed model is 40.89 and 39.96% in the same earthquake.

Normally, when base isolators are applied in orthogonal direction, it is expected that the response of structures will be mitigated. However, the shear forces of BI-NPPs are significantly larger than the fixed base model. The results show that it is important to consider the IA when applying isolator to structure to design more accurate isolator system.

Critical angle

In order to investigate the effects of the bi-directional ground motion on the NPPs, the displacement at the top node and shear force at element 5701 are considered. For each angle, the responses to the orthogonal seismic components at a time instant t were computed by Equations (3)–(9) in Chapter 4.

Displacement

One of the most important criteria of EDPs is the displacement at the top of NPPs structure. Figure 10 shows the critical displacements of structure under Loma Prieta and Imperial Valley ground motions. Under Loma Prieta, the maximum displacement $u_{max} = .0476$ m is obtained at time instant $t_{cr} = 4.43$ sec. At the same time, the value of displacements due to excitation at x and y is $u_x = .0108$ m and $u_y = -.0464$ m, respectively. Using the Equation (5), the critical angles of the structure are 283.13° for maximum and 103.13° for minimum response under Loma Prieta earthquake. Similarly, maximum response under Imperial Valley at time instant $t_{cr} = 14.32$ sec is six times higher than under Loma Prieta. The critical angles for the maximum and the minimum response are 75.74° and 255.74°, respectively. The values of displacements are $u_x = .0159$ m and $u_y = -.0422$ m along x, y direction, respectively.

Shear force

Figure 11 displays the data of critical shear force of structure under Loma Prieta and Imperial Valley earthquakes. The critical shear force under Imperial Valley is larger approximately four times than Loma Prieta, which is only 2.03×10^8 N. The critical angles are 32.20°, 212.20° for Loma Prieta and 328.92°, 148.92° for Imperial Valley earthquake records.

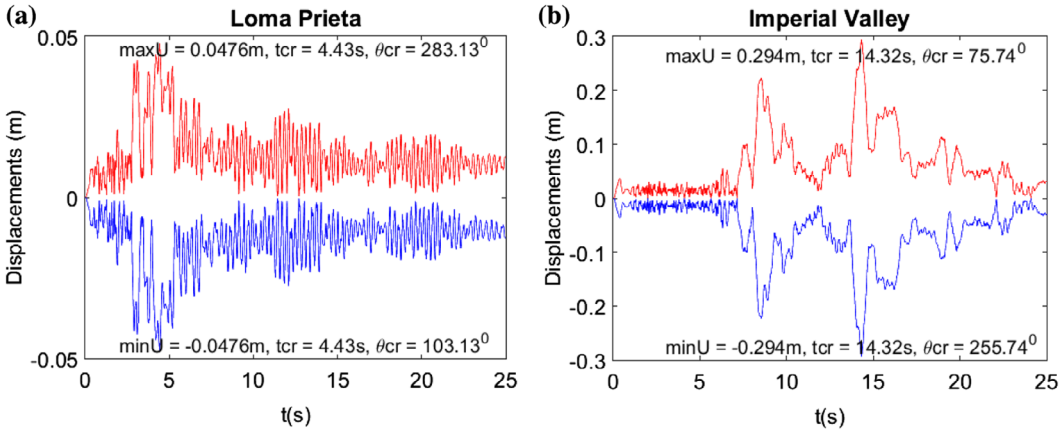

Figure 10. Critical displacement under different earthquakes.

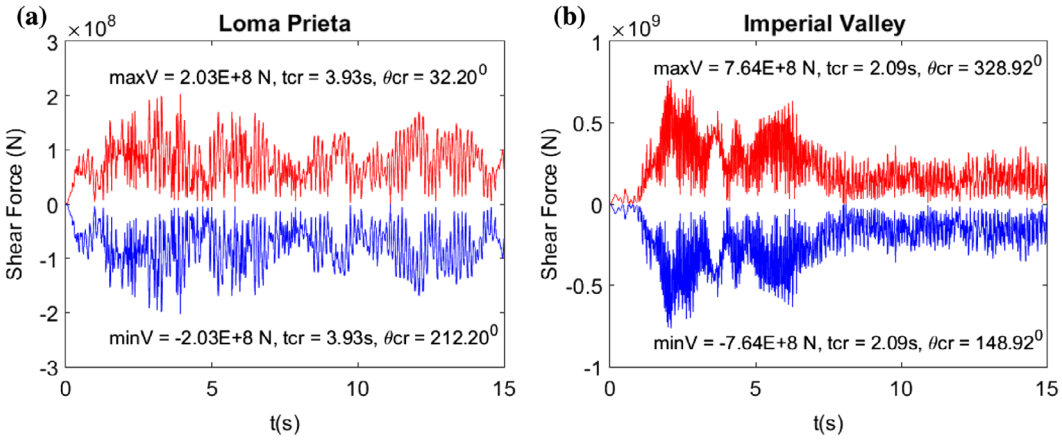

Figure 11. Critical shear force under different earthquakes.

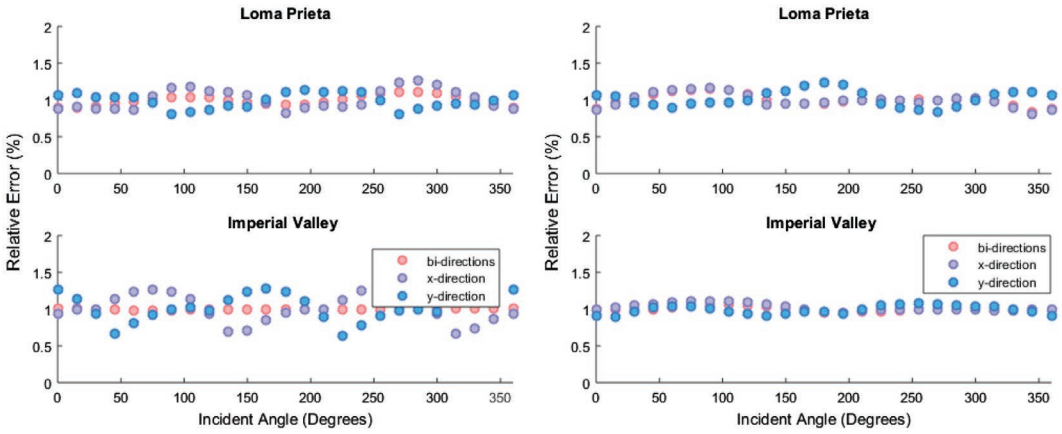

a) Displacement b) Shear Force

Figure 12. Relative errors of incidence angle under different earthquakes.

Effect of IA to EDPs

To clarify the impacts of IA when horizontal accelerations applied separately (the purple and blue dots) and simultaneously (the red dots), the relative error which is calculated by Equations (10)–(12) is used. The relative errors are illustrated in Figure 12. Generally, it can be observed that effects of earthquake incident on bi-direction are less considerable than uni-directional. The displacement and shear force of Imperial Valley in case of two directions seem stable under different angles, while there is strong variability in case of one direction.

For a better comparison, the relative errors of displacement are shear force are presented in Figure 13. Comparing the bottom and top values of the boxes that defined 25 and 75% percentiles, it can be seen that the relative differences in case of each direction are larger than two directions. In addition, maximum and minimum values of relative differences are also greater in case of each direction under different ground motion records. Table 3 shows the effects of single and double directions under seismic excitations. In particular, the effect is not too much different to shear force of two ground motion

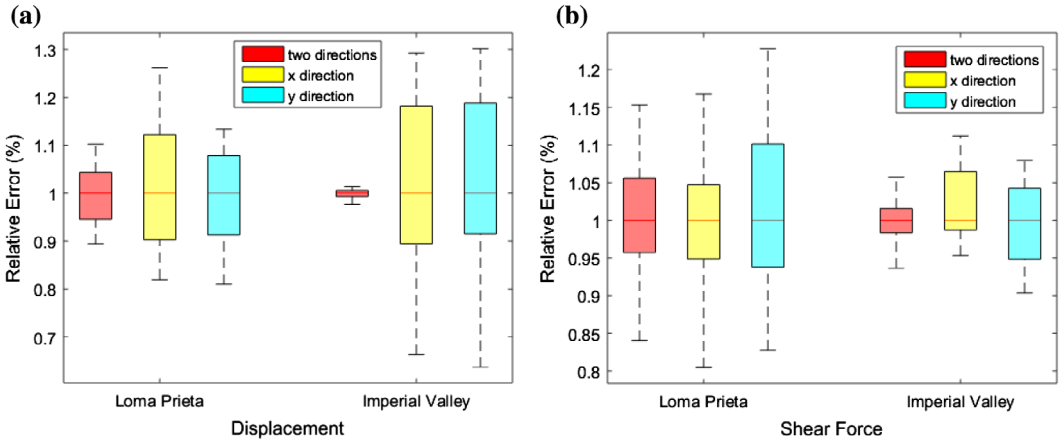

Figure 13. Relative errors of analysis – boxplots.

Table 3. Maximum relative deviation of responses (%).

		Displacement	Shear force
EUR	Two directions	23.29	37.22
	X direction	54.09	45.12
	Y direction	40.02	48.34
NRC	Two directions	3.74	12.88
	X direction	94.97	16.68
	Y direction	104.27	19.48

records. However, the maximum relative deviation of displacement response of Imperial Valley of two directions is only 3.74%, while in case of each direction the values are 94.97 and 104% for *x* and *y* directions, respectively. The above results demonstrate that when considering earthquake incidence, the response of the structure under two components might be less than one component.

Conclusion

In this study, the IA effect of ground motion on seismic parameters of the BI-NPPs structure supported by one-bearing equivalent is investigated. The ground motion inputs are applied considering both uni-directional and bi-directional components. Based on the obtained results, the major conclusions can be drawn as follows:

- The responses obtained from isolated structure under bi-directional ground motions are greater than responses produced by uni-directional earthquake. The different gap of maximum responses under two components is less than corresponding results under one component.
- The critical angle under two ground motion components in structural behavior differs from one component. The critical angle of the BI-NPPs structure tends to occur when two horizontal acceleration components are applied at non-orthogonal direction. The variability of the critical angle for each response of displacement and shear force could be obtained at the variable time instant at different angles. The maximum displacement at the time instant is 4.43s and 14.32s under Loma Prieta and Imperial Valley, respectively.
- The maximum relative variation confirms that the structural responses, depending on one or two horizontal directions involved. The deviation ratios under two horizontal directions show better than one direction. For the BI-NPPs structure of a bi-directional seismic input, the maximum relative deviations of displacement response are 3,74 and 23.29% under Imperial Valley and Loma Prieta earthquake, respectively.
- Also, the correlation between IA of ground motion and isolator system is also depicted. In some cases, the responses of BI-NPPs are more significant than the fixed NPPs model. There are increasing amounts of displacement from .0164 to .0407 m and from .0160 to .0463 m for each direction under Loma Prieta; for Imperial Valley these values change from .016 to .210 m and from .0160 to .0283 m in *x* and *y* directions, respectively. However, there is minor effect in the relative displacements of superstructure. Therefore, it is important to underline that the influence of the characteristics of the structures should be considered in the seismic design.

Disclosure statement

No potential conflict of interest was reported by the authors.

Funding

This work was supported by the National Research Foundation of Korea (the Korean Government) [grant number NRF-2018R1A2B2005519].

References

Ali, A., Abu-Hayah, N., Kim, D., & Cho, S. G. (2017). Design response spectra-compliant real and synthetic GMS for seismic analysis of seismically isolated nuclear reactor containment building. *Nuclear Engineering and Technology, 49*(4), 825–837.

Ali, A., Hayah, N. A., Kim, D., & Cho, S. G. (2014). Probabilistic seismic assessment of base-isolated NPPs subjected to strong ground motions of Tohoku Earthquake. *Nuclear Engineering and Technology, 46*(5), 699–706.

Athanatopoulou, A. M. (2005). Critical orientation of three correlated seismic components. *Engineering Structures, 27*(2), 301–312.

Chang, S., Sun, W., Cho, S. G., & Kim, D. (2016). Vibration control of nuclear power plant piping system using stockbridge damper under earthquakes. *Science and Technology of Nuclear Installations,* 2016.

EUR. (2002). E. U. R. European utility requirement for LWR nuclear power plants. *EUR European Utility Requirement for LWR Nuclear Power Plants*.

Ghersi, A., & Rossi, P. P. (2001). Influence of bi-directional ground motions on the inelastic response of one-storey in-plan irregular systems. *Engineering Structures, 23*(6), 579–591.

Heredia-Zavoni, E. (2011). The complete SRSS modal combination rule. *Earthquake Engineering and Structural Dynamics, 40*(11), 1181–1196.

Hernández, J. J., & Lopez, O. A. (2003). Evaluation of combination rules for peak response calculation in three-component seismic analysis. *Earthquake Engineering & Structural Dynamics, 32*(10), 1585–1602.

Kim, D., Wang, F., & Chaudhary, S. (2016). Modal energy balance approach for seismic performance evaluation of building structures considering nonlinear behaviour. *Journal of Structural Integrity and Maintenance, 1*(1), 10–17.

Kostinakis, K. G., Athanatopoulou, A. M., & Tsiggelis, V. S. (2013). Effectiveness of percentage combination rules for maximum response calculation within the context of linear time history analysis. *Engineering Structures, 56*, 36–45.

Lagaros, N. D. (2010). The impact of the earthquake incident angle on the seismic loss estimation. *Engineering Structures, 32*(6), 1577–1589.

Lopez, O. A., Chopra, A. K., & Hernandez, J. J. (2000). Critical response of structures to multicomponent earthquake excitation. *Earthquake Engineering & Structural Dynamics, 29*(12), 1759–1778.

López, O. A., & Torres, R. (1997). The critical angle of seismic incidence and the maximum structural response. *Earthquake Engineering & Structural Dynamics, 26*(9), 881–894.

Menun, C., & Kiureghian, A. D. (2000a). Envelopes for seismic response vectors. I: Theory. *Journal of Structural Engineering, 126*(4), 467–473.

Menun, C., & Kiureghian, A. D. (2000b). Envelopes for seismic response vectors. II: Application. *Journal of Structural Engineering, 126*(4), 474–481.

Nguyen, V. T., & Kim, D. (2013). Influence of incident angles of earthquakes on inelastic responses of asymmetric-plan structures. *Structural Engineering and Mechanics, 45*(3), 373–389.

Penzien, J., & Watabe, M. (1974). Characteristics of 3-dimensional earthquake ground motions. *Earthquake Engineering & Structural Dynamics, 3*(4), 365–373.

Rigato, A. B., & Medina, R. A. (2007). Influence of angle of incidence on seismic demands for inelastic single-storey structures subjected to bi-directional ground motions. *Engineering Structures, 29*(10), 2593–2601.

Sayed, M. A., Go, S., Cho, S. G., & Kim, D. (2015). Seismic responses of base-isolated nuclear power plant structures considering spatially varying ground motions. *Structural Engineering and Mechanics, 54*(1), 169–188.

Sharmin, F., Hussan, M., Kim, D., & Cho, S. K. (2017). Influence of soil-structure interaction on seismic responses of offshore wind turbine considering earthquake incident angle. *Earthquakes and Structures, 13*(1), 39–50.

Smeby, W., & Der Kiureghian, A. (1985). Modal combination rules for multicomponent earthquake excitation. *Earthquake Engineering & Structural Dynamics, 13*(1), 1–12.

Soltani, M., Shakeri, E., & Zarrati, A. R. (2018). Development of a risk management model for power tunnels design process. *Journal of Structural Integrity and Maintenance, 3*(1), 67–74.

Tsourekas, A. G., & Athanatopoulou, A. M. (2013). Evaluation of existing combination rules for the effects caused by three spatial components of an earthquake. *KSCE Journal of Civil Engineering, 17*(7), 1728.

Tyapin, A. G. (2016). Damping in the platform models for soil-structure interaction problems: Rayleigh damping options and limitations in modal analysis. *Journal of Structural Integrity and Maintenance, 1*(3), 114–123.

US Nuclear Regulatory Commission. (1973). *Regulatory Guide 1.60: Design response spectra for seismic design of nuclear power plants*. Washington, DC: US Atomic Energy Commission. Retrieved April 2012 from http://pbadupws.nrc.gov/docs/ML1335/ML13350A358.pdf

Valdés-González, J., Schroeder, M. O., & Martínez, J. D. L. C. (2015). Combination rule for critical structural response in soft soil. *Engineering Structures, 82*, 1–10.